Dynamics of analyte binding onto a metallophthalocyanine: NO/FePc

Sarah R. Bishop,[a] Ngoc L. Tran, Gary C. Poon, and Andrew C. Kummel
Department of Chemistry and Biochemistry, University of California, San Diego, La Jolla, California 92093-0358, USA

(Received 27 June 2007; accepted 9 October 2007; published online 4 December 2007)

The gas-surface reaction dynamics of NO impinging on an iron(II) phthalocyanine (FePc) monolayer were investigated using King and Wells sticking measurements. The initial sticking probability was measured as a function of both incident molecular beam energy (0.09–0.4 eV) and surface temperature (100–300 K). NO adsorption onto FePc saturates at 3% of a monolayer for all incident beam energies and surface temperatures, suggesting that the final chemisorption site is confined to the Fe metal centers. At low surface temperature and low incident beam energy, the initial sticking probability is 40% and decreases linearly with increasing beam energy and surface temperature. The results are consistent with the NO molecule sticking onto the FePc molecules via physisorption to the aromatics followed by diffusion to the Fe metal center, or precursor-mediated chemisorption. The adsorption mechanism of NO onto FePc was confirmed by control studies of NO sticking onto metal-free H_2Pc, inert Au(111), and reactive Al(111). © *2007 American Institute of Physics*. [DOI: 10.1063/1.2804870]

I. INTRODUCTION

Metallophthalocyanines (MPc) are employed for use in organic-based chemical field effect transistors for the measurement of gas phase analytes such as NO, NO_2, and O_3.[1–4] The molecular structure of one such MPc, FePc, is shown in Fig. 1. While the films have been extensively studied by low energy electron diffraction (LEED), scanning tunneling microscopy (STM), scanning tunneling spectroscopy, and current imaging tunneling spectroscopy on various substrates,[5–10] there are no reported measurements probing the reaction dynamics using molecular beams on either ordered monolayer or multilayer films. In general, the roles of the aromatic rings and the metal center for chemisorption and physisorption of gas molecules are unknown. The literature provides contrasting opinions as to whether chemisorption occurs on the organic rings or to the metal center.[11] A previous study using a thermal desorption technique verified that NO can chemisorb to FePc through the observation of NO/FePc desorption spectra with a high temperature peak at 100–250 °C.[12] This is consistent with NO strongly bonding with electron rearrangement to FePc. While this study proved that NO chemisorbs to FePc, the interrelationship between physisorption and chemisorption of NO on FePc and the site of the two adsorption processes could not be ascertained.

The relationship between the chemisorption and physisorption sites on the surface is critical to the chemical dynamics of NO with the FePc surface. Physisorption prior to chemisorption is denoted as precursor-mediated chemisorption.[13–15] In this mechanism, the gas phase adsorbate traps into a precursor state and can either adsorb onto the chemisorption site by overcoming a reaction barrier or desorb back into the gas phase. Direct chemisorption can be distinguished from precursor-mediated mechanism by analyzing the dependence of the initial sticking probability S_0 on the sample temperature T_s and the incident energy of the molecular beam E_i. If S_0 is strongly dependent on T_s and E_i, the mechanism is typically precursor-mediated chemisorption. This is due to the decreasing ability of the analyte to trap into the shallow physisorption wells as the surface's energy is increased via T_s or the molecule's energy is increased via E_i. Previous studies have shown S_0 dependence on both T_s and E_i for many precursor-mediated chemisorption systems.[16–19]

NO chemisorption onto metal surfaces is known to occur by a variety of mechanisms.[16,20–24] One study shows that initial adsorption of NO onto Pt(111) has a monotonic sticking decrease from 90% to 20% as the incident beam energy is increased.[16] Although NO physisorbs N end down, the sticking probability above 50% at low temperature and low beam energy is attributed to a rotational steering effect and is assisted by a diversity of adsorption sites.[25] The diversity of adsorption sites can be deduced from the LEED pattern as a function of coverage for NO/Pt(111). At 110 K, NO forms a (2×2) structure on Pt(111) from coverages of 0.25 to 0.75 ML, indicating both ordered and disordered adsorption sites.[26] While there is a general understanding of NO interaction with single crystal surfaces, the literature lacks an investigation of NO adsorption dynamics with more complex surfaces, such as FePc thin films.

In the current study, the S_0 of NO on FePc was measured as a function of T_s and E_i using the King and Wells reflection technique.[27,28] The heterogeneity of the FePc surface (metal center, surrounding pyrrole and *meso* nitrogen atoms, and four equivalent aromatic rings) adds complexity to the chemisorption process. The distinct roles played by both regions, metallic and organic, of the FePc molecule were determined via sticking probability experiments onto metal-

[a]Electronic mail: sbishop@ucsd.edu

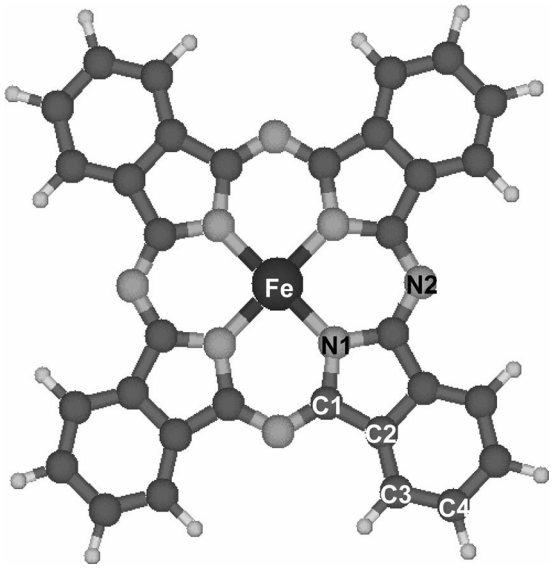

FIG. 1. A ball-and-stick diagram used to depict the atoms of the FePc molecule. Adsorption sites labeled.

free phthalocyanine (H_2Pc), inert Au(111), and reactive Al(111) in addition to the monolayer FePc.

II. EXPERIMENTAL PROCEDURE

The UHV reaction chamber used in this study has been described previously.[29,30] The chamber is equipped with an Auger electron spectroscope (AES), LEED, a quadruple mass spectrometer, an Ar^+ ion sputter gun, an effusion cell for FePc deposition, and a supersonic molecular beam, as depicted in Fig. 2. The clean single crystal Au(111) sample was prepared by 2 kV Ar^+ sputtering for 20 min followed by annealing the sample to a surface temperature (T_s) of 775 K for 5 min. The sample was slowly (1 K/s) cooled to 675 K followed by rapid cooling (~5 K/s) to 300 K. The order of the surface was checked by LEED at 51 eV and consistently found to be the expected $\sqrt{3}\times 22$ hcp reconstruction. Surface cleanliness was checked by AES, which verified that only Au was present.

The monolayer FePc was formed on the Au(111) surface using a "top down" approach in which a thick overlayer of FePc was first sublimated onto the room temperature substrate. A low temperature effusion cell (Createc LTC-40-20-SH-M) was used for the deposition process; the FePc multilayer was deposited by maintaining the cell temperature

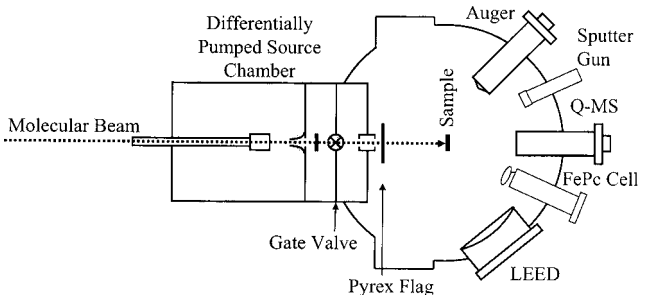

FIG. 2. A schematic of the UHV reaction chamber used in this experiment is shown. LEED, Auger, and the effusion cell are labeled.

at 615 K for 2 min. Subsequently, the thick overlayer was partially evaporated from the Au(111) surface by increasing the substrate temperature to 625 K for 2 min. This process leaves a flat-lying monolayer of FePc on the Au(111) surface. This partial evaporation technique is successful due to the FePc/substrate interaction being stronger than the FePc/FePc interaction.[31]

AES measurements of the annealed FePc film exhibited a C to N ratio of 4:1, along with a residual Au peak, consistent with a monolayer of intact FePc. Conversely, for multilayer films, the residual Au peak is no longer present. The order of the FePc monolayer was checked with LEED at 15 eV to verify observation of the signature MPc/Au(111) diffraction pattern containing a superposition of three rotationally equivalent domains.[32] The Au(111) $\sqrt{3}\times 22$ hcp reconstruction spots were still visible at 51 eV for monolayer FePc films, while they were not observed for the multilayer films. STM of monolayer CuPc on Au(111), prepared using similar sample preparation and deposition techniques in another apparatus in our laboratory, showed monolayer CuPc lying parallel to the Au(111) plane as observed by other groups on similar systems.[31–33] Flat-lying MPc films are an essential part of this study since they ensure that both the Fe metal and aromatics are exposed and readily available for NO adsorption. The Auger, LEED, and STM studies along with previously reported studies on preparation of MPc films confirm that our annealed FePc films contain 1 ML of intact FePc molecules.

During sticking measurements, the temperature of the sample was maintained by simultaneous liquid nitrogen cooling and radiative heating from the back side of the sample with an iridium ribbon filament. The sample temperature was varied from 100 to 300 K in 25° increments. The incident beam translational energy (E_i) was varied via seeding the pure NO beam with He or Ne. These energies were calculated as described previously by Haberland *et al.*,[34] resulting in the following values: 0.09 eV, 0.26 eV, and 0.4 eV for 20% NO in Ne, 20% NO in He, and 5% NO in He, respectively. These values agree with experimental data for beams of similar concentration and mass mismatch reported by other groups.[35] Previous experiments, performed using the same chamber as this study, determined the translational beam energy for molecular beams of seeded CO using a fast resonantly enhanced multiphoton ionization detection system.[36] The molecular beams studied are comparable to the gas concentrations and mass differences between the NO and seed gases employed in the present study. In addition, the velocity slip is a negligible effect for the molecular beams in this study. This was determined theoretically via methods described by Tsipinyuk *et al.* in which their beams have a larger mass ratio than the ones for this experiment.[37,38]

To perform King and Wells experiments with a molecular beam of a reactive analyte, such as NO, it is necessary to passivate the chamber with the gas to occupy any available adsorption sites on the chamber walls.[24,39] To chemically passivate the chamber walls, the molecular beam of NO was directed onto a Pyrex flag in the UHV reaction chamber for 1 h while the sample was cooled to liquid nitrogen temperature (<100 K). After wall passivation, but prior to the ex-

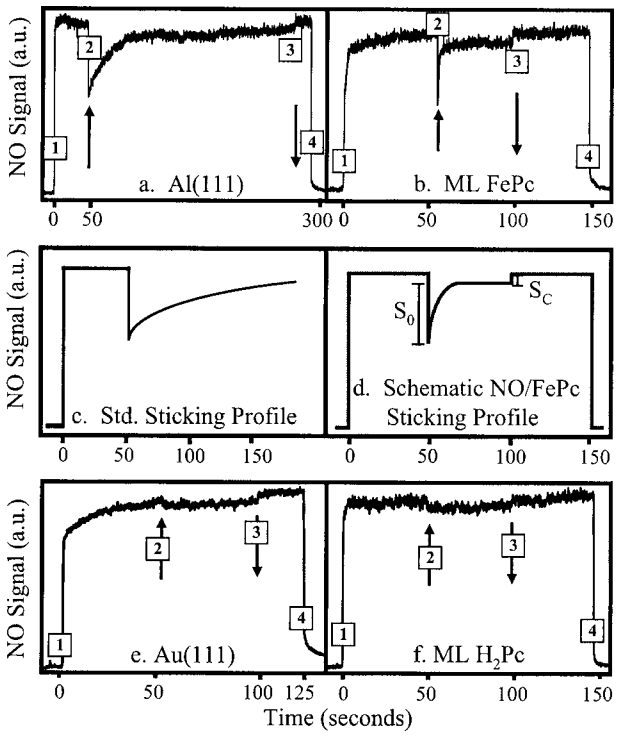

FIG. 3. The comparison of NO interaction with (a) Al(111), (b) monolayer FePc, (c) schematic of standard sticking, (d) schematic of monolayer FePc sticking, (e) Au(111), and (f) monolayer H_2Pc is depicted via King and Wells sticking profiles. The NO signal is equivalent to the partial pressure of NO during the experiment. "Profile a" is a sample sticking profile of a 0.09 eV NO beam impinging onto an Al(111) surface at 300 K. "Profile b" is a sample profile of a 0.09 eV beam impinging on a monolayer FePc surface at 150 K. "Profile c" is a representation of a standard Langmuirian sticking profile, modeled after profile a. This is in comparison to "profile d," a representation of the monolayer FePc sticking profile b. Note the time scale differences between profiles a and b. The initial sticking S_0 and sticking due to the contaminant, S_c, are labeled in profile d. "Profile e" is a sample sticking profile of a 0.09 eV NO beam impinging on a clean Au(111) at 150 K. "Profile f" is a sample sticking profile of a 0.09 eV NO beam impinging onto monolayer H_2Pc at 200 K. Note the similarities to the sticking profile e. The experimental procedure is labeled for the profiles with numbers. (1) Gate valve open, (2) flag open, (3) flag closed, and (4) gate valve closed. The time scale of the experiment is labeled along with arrows denoting the opening (up arrow) and closing (down arrow) of the Pyrex flag during the experiment. The gradual surface saturation of Al(111) surface is different than the short saturation time of the monolayer FePc surface. Note the sharp downward spike upon flag removal in profile b.

periment, the molecular beam was blocked by a gate valve between the molecular beam source and the UHV chamber, and any NO on the surface was removed via flash annealing to 375 K. The normal sequence of valve and flag operation employed for the sticking measurement includes the following (see Fig. 3): (1) the gate valve was opened with the flag in front of the sample resulting in an immediate pressure rise; (2) after the partial pressure of NO has stabilized, the flag was removed, and the NO partial pressure versus time was recorded until absorption was saturated; (3) the flag was repositioned again in front of the sample, and the partial pressure of NO at equilibrium was again recorded to check that the NO beam flux was stable; and (4) the gate valve was closed. The initial sticking probability is calculated from the sticking curves by taking the ratio of the immediate partial pressure drop upon flag removal over the equilibrated partial pressure rise upon opening the gate valve. The sequence of measurements is shown in Fig. 3, including (a) NO/Al(111), which exhibits a typical sticking versus time profile for chemisorption on a metal surface, and for (b) NO/FePc, which exhibits a unique sticking versus time profile.

It is important to note that the highly reactive nature of NO gas can lead to the formation of a small amount of contaminant in the gas regular over time. These contaminants result in the steady state sticking, S_c, of approximately 2%–4%, as seen in Fig. 3. This 2%–4% steady state sticking is due to contaminant condensation and is substrate independent. While molecular NO does not condense between 100 and 300 K, it might stick to the condensation layer of contaminant on the substrate. Even though the effects of the contaminants are negligible for the initial sticking probabilities, the influence of the contaminants on NO sticking was corrected by subtracting the percentage of steady state sticking from the initial sticking.

III. RESULTS AND DISCUSSION

A. Initial sticking data

1. NO interaction with inert Au(111)

Prior to performing sticking measurements of NO on FePc, it is necessary to verify that NO only interacts with the FePc surface and not the Au(111) substrate. To confirm that NO is sticking only to the FePc molecule, sticking probability measurements were performed on the clean Au(111) surface. Figure 3(e) shows that the sticking profile of NO onto Au(111) is zero at 150 K. Similar results were observed for all sample temperatures between 100 and 300 K. This indicates that the Au(111) substrate does not provide any viable adsorption sites. These results are consistent with a previous study showing that the binding energy for NO on Au(111) is 0.5–0.8 eV at 300 K; consequently, the surface residence time for NO/Au(111) is less than 30 μs at 300 K.[40] These results confirm that any adsorbate sticking on FePc/Au(111) is a direct result of NO/FePc interactions. Therefore, the Au(111) acts only as an inert support substrate for the FePc film.

2. NO initial sticking on FePc thin films versus T_s and E_i

The NO/FePc/Au(111) sticking profile sharply contrasts with the NO/Al(111) sticking profile [Fig. 3(b)]. The unique feature in the NO/FePc sticking profile at low temperature is a sharp downward spike with a fast recovery lasting 1–2 s. The term "sharp downward spike" will be used throughout the manuscript and to denote the very short NO/FePc sticking profiles in comparison to the standard slower sticking profile observed in King and Wells sticking experiments. The instantaneous downward spike for NO/FePc(111) occurs immediately after the flag is removed from the molecular beam path and is most prominent at low T_s and E_i. The area of the sharp spike represents total NO adsorption onto the monolayer FePc surface. It is expected that only the metal centers are available for chemisorption; therefore, saturation should occur very rapidly for NO/FePc compared to NO/Al(111). As shown in Fig. 4, the width of the NO/FePc sharp downward spike varies with tempera-

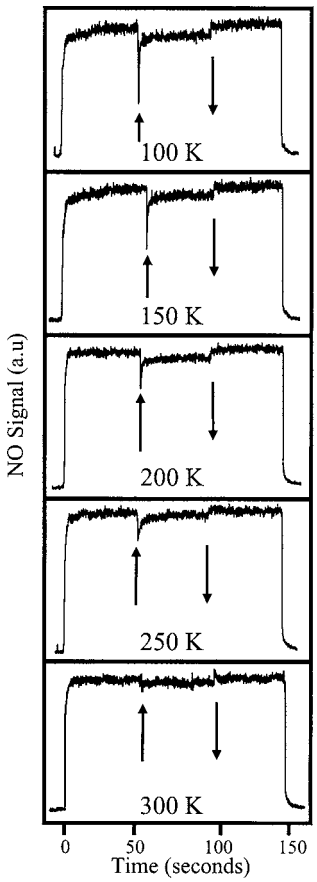

FIG. 4. A collection of sample sticking profiles of a 0.09 eV NO beam impinging onto monolayer FePc for a range of temperatures (100–300 K). The arrows represent the removal and replacement of the flag during the experiment. An interesting feature is the sharp downward spike upon flag removal, seen most prominently at low temperatures.

ture; as T_s increases, the width of the downward spike also increases, which is representative of an increase in the time to saturation. While the width of the downward spike increases, the S_0 decreases, maintaining a nearly constant area within the downward spike. This behavior is expected because the available number of chemisorption sites remains constant as the other variables of the experiment are adjusted.

The initial sticking probability versus sample temperature for varying incident beam energies of NO on monolayer FePc/Au(111) is plotted in Fig. 5. The initial sticking probability S_0 is 40% at T_s=100 K and E_i=0.09 eV and decreases linearly with increasing surface temperature. The decrease of S_0 with increasing T_s, for all incident beam energies, is consistent with the decreasing probability of NO trapping into shallow-well physisorption sites and subsequently chemisorbing to the metal center at increasing temperature.

Figure 6 is a plot of S_0 versus E_i for varying surface temperatures. As E_i increases, the initial sticking decreases monotonically, consistent with trapping into a shallow physisorption well prior to chemisorption to the metal center, or precursor-mediated chemisorption. As the temperature increases to 300 K, the desorption temperature of NO on FePc, S_0 approaches 0% for all three incident beam energies studied. If NO adsorption to the surface could be described by direct chemisorption, the initial sticking probability should be independent of E_i. Therefore, based on the E_i dependence, the NO sticking mechanism is consistent with precursor-mediated chemisorption.

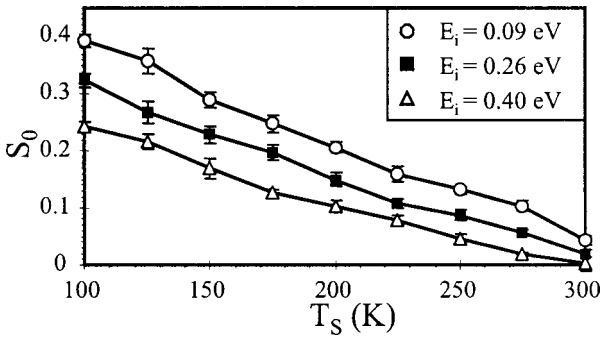

FIG. 5. Initial sticking probability of NO on monolayer FePc films as a function of sample temperature for varying incident beam energies (0.09–0.40 eV). The solid lines reflect the sticking probability gradual dependence on surface temperature. Standard errors are indicated via error bars.

3. NO sticking on metal-free H_2Pc

Measurement of NO sticking onto H_2Pc was performed to identify the roles of the organic periphery in the absence of a metal. Figure 3(f) shows a King and Wells sticking curve for NO/H_2Pc. There is no measurable sticking in the temperature range studied for NO onto the H_2Pc surface, similar to the results of NO impinging on the clean Au(111) surface. The lifetime of the NO molecule on H_2Pc can be estimated using the same method as that of Wodkte *et al.* along with the NO binding energies (0.2 eV) to the organic periphery calculated by Tran and Kummel.[40,41] The lifetimes of the NO molecule on H_2Pc were estimated to be 20 ms and 0.01 μs at 100 and 300 K, respectively. Conversely, our experiments show that the lifetime of the NO molecule on FePc is infinite compared to the time scale in the scope of this experiment between 100 and 300 K. Without a metal center in the phthalocyanine molecule, no chemisorption of the analyte to the surface occurs. Therefore, the metal center is the only chemisorption site for the precursor-mediated sticking mechanism.

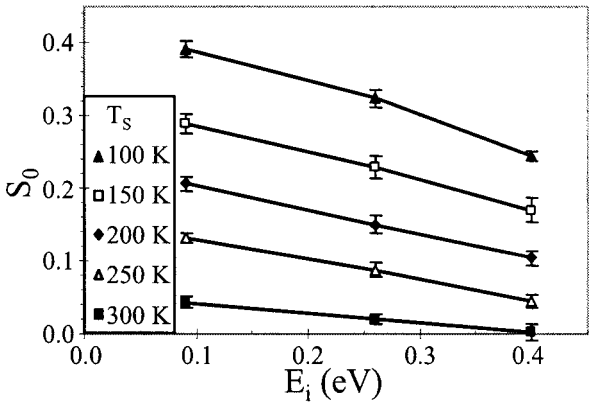

FIG. 6. Initial sticking probability as a function of incident beam energy for varying sample temperatures (100–300 K) for NO on monolayer FePc.

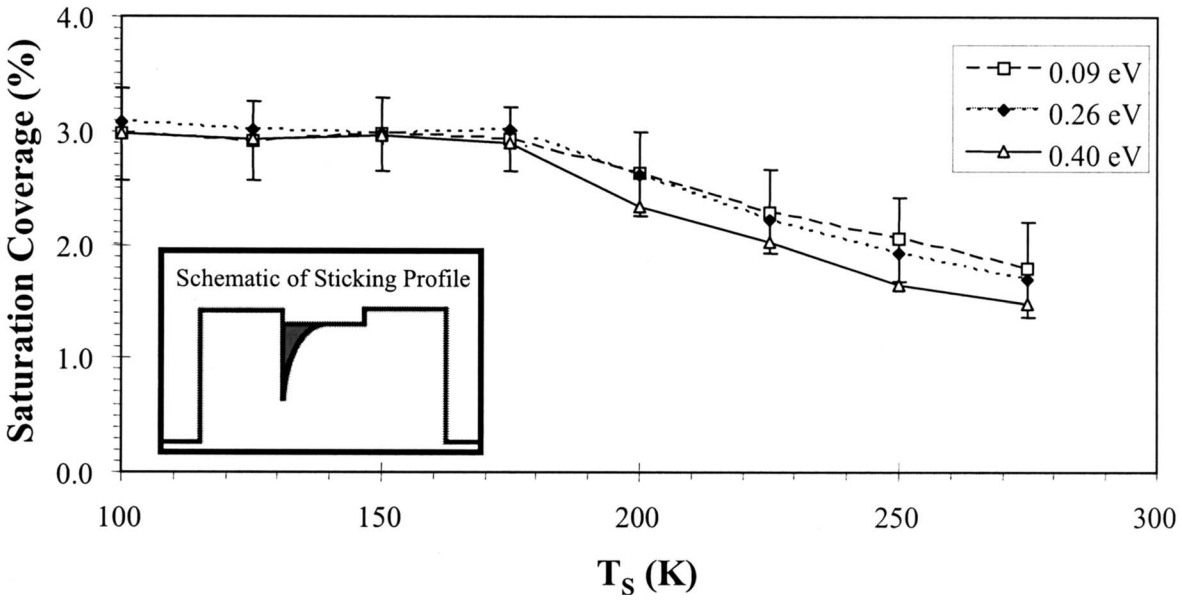

FIG. 7. NO saturation coverage as a function of sample temperature and incident beam energy. Inset demonstrates method of calculation of the saturation coverage from the initial sticking profile data via measurement of the area in the spike.

4. Saturation coverage of NO on monolayer FePc

In addition to the initial sticking probabilities, the normalized surface coverage of NO saturation on monolayer FePc was calculated. Using the covalent radius of Fe, 1.17 Å, to estimate a capture cross section, the total surface area the Fe metal centers occupy in the thin film is about 3% of a monolayer.[42] Therefore, a low saturation coverage is expected if chemisorption is restricted to the metal centers. To determine the saturation coverage of NO on FePc experimentally, the flux of NO must be quantified. The flux of NO was measured using the same molecular beam and recording the sticking as a function of time for NO on Al(111), since it is known that NO has a saturation coverage of 1 ML on Al(111).[23] The normalized saturation coverage was determined via comparison of the integrated area of the sharp spike from the NO/FePc sticking profiles to the integrated area within the NO/Al(111) sticking curve. It should be noted that the NO/FePc and NO/Al(111) experiments were performed with identical experimental conditions to ensure identical fluxes and pumping speeds.

Figure 3(a) depicts typical sticking of NO/Al(111) with S_0=40% (note that the x axis has a different scale than for the FePc experiments). The initial sticking is followed by a 100 s gradual surface saturation that can be modeled via simple Langmuirian adsorption. The NO/Al(111) sticking results are consistent with previously reported experiments.[23,43] The saturation time for NO on the Al(111) surface is 30 times longer than that for NO/FePc. This is attributed to the increase in available chemisorption sites on the Al(111) surface compared to monolayer FePc.

The inset in Fig. 7 shows a schematic of the sticking profile. The area of the sharp downward spike was calculated by simple integration. As previously discussed, contributions from the contaminant to the area of the sharp spike were removed. The plot in Fig. 7 shows the normalized NO saturation coverage as a function of sample temperature for the three incident beam energies studied. The calculation shows that the maximum total surface coverage of NO on monolayer FePc is 3% ML for all three incident beam energies from 100 to 175 K. The 3% ML saturation coverage is identical to the 3% ML area comprised of the Fe metal centers on the FePc monolayer. From 200 to 300 K, the total saturation coverage decreases for all three incident beam energies. This is attributed to both the approach of the NO desorption temperature and the lack of accuracy in the measurement of the area within the spike for the sticking profiles with low sticking probabilities. These results are consistent with the NO/FePc versus NO/H_2Pc results indicating that the only available chemisorption site on the surface is the iron metal center. The aromatics act as a precursor site prior to diffusion to the chemisorption site.

Under optimal conditions, the sticking versus time data can also be employed to determine the effect of NO–NO interactions on sticking, a type of coadsorbate interaction. Coadsorbates can simply block adsorption sites or they can cause a delocalized perturbation of the chemisorption dynamics via coadsorbates donating or accepting charge, thereby changing gas adsorption energies.[44–46] For noninteracting molecular chemisorption sites, the sticking probability should scale with the number of available sites, $(1-\theta)$. Since the saturation coverage is only 0.03 ML for the current study, the saturation time is so short that the data are insufficient to distinguish modest deviations from $(1-\theta)$ scaling. However, the MPc electronic structure is completely localized to each MPc molecule; therefore, the chemisorption of NO on a given MPc molecule is expected to be independent of the chemisorption of NO on a neighboring MPc molecule.[41]

B. Multiple precursor-mediated chemisorption mechanism model

At T_s=100 K, S_0 for NO/FePc/Au(111) is at least ten times greater than the 3% surface area available for chemi-

sorption. However, the high sticking probability, 40%, is consistent with available physisorption sites on the aromatic portions of the FePc molecule. Using the covalent radius of the atoms in the FePc molecule, we estimate that the area available for physisorption for NO/FePc accounts for approximately 60% of the total FePc/Au(111) unit cell. Therefore, it is reasonable to observe a sticking probability of 40% at our lowest beam energy at 100 K. Based on the linear dependence of S_0 on T_s it is postulated that as T_s decreases, S_0 should approach 60% below 100 K. This is consistent with NO being able to trap onto all the physisorption sites, C and N atoms, within the FePc molecule. On metallic single crystals, the intrinsic precursor and chemisorption sites are usually identical atoms. However, on the heterogeneous FePc surface, the physisorption and chemisorption sites are different. The high sticking probability for low saturation coverage is consistent with the availability of C and N sites in the aromatics for NO physisorption prior to diffusion to the metal center.

Complementary density functional theory (DFT) geometry relaxation calculations were performed for the NO on FePc system to elucidate the details of the chemisorption mechanism.[41] The total adsorption energy was calculated by placing NO at various sites on the FePc molecule. The DFT calculations showed that although only the metal center sites had a NO adsorption energy typical of chemisorption (−1.7 eV), there were multiple organic sites with adsorption energies consistent with physisorption (−0.2 eV). The simulations show barrierless NO diffusion from the inner ring N to the metal center, and small barriers between the other peripheral physisorption sites. It should be noted, however, that DFT simulations do not predict van der Waals interactions accurately. While the chemisorption energies are reliable, the physisorption well depths tend to be underestimated. The physisorption sites were sufficiently shallow to be consistent with decreasing sticking probability with increasing molecular beam energy and increasing surface temperature. As the temperature of the sample increases or the energy of the incident beam energy increases or the surface temperature increases, the analyte's ability to trap and diffuse to the chemisorption site is reduced, with the magnitude of reduction differing depending on the physisorption site.

To verify the existence of multiple physisorption sites with a diversity of NO physisorption well depths, the relative activation barriers for desorption versus diffusion from the physisorption sites were calculated. Upon trapping to the aromatic periphery, the NO molecule can either overcome a small barrier to diffuse to the Fe center or a barrier to desorb from the surface. The standard analysis assumes that the primary effect of raising T_s is upon the partitioning between diffusion and desorption instead of upon the trapping probability into the physisorption state. Furthermore, standard treatment of the initial sticking data is not possible using the Arrhenius equation due to the complicated nature of the multiple precursor-mediated mechanisms for NO chemisorption to the metal center.[17,47,48] When the initial sticking data are plotted via the Arrhenius equation, the slope of the line represents the difference in the activation barriers to desorption compared to chemisorption; however, in this study, the line is not linear. Nonlinearity in the Arrhenius plot suggests that there exist multiple barriers to desorption/chemisorption on the heterogeneous surface for NO that were defined by the slopes of the curve. By treating the experimental data using rate coefficients k (the Polanyi-Wigner form), it can be deduced to

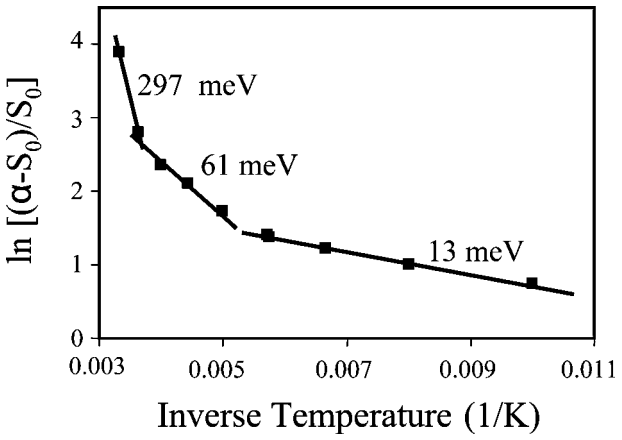

FIG. 8. A sample Arrhenius plot used to determine the activation barriers of NO chemisorption upon physisorption. The sticking data plotted are for E_i =0.26 eV; however, all three beam energies had the same curve. The result is a nonlinear relationship between $\ln[(\alpha\text{-}S_0)/S_0]$ and inverse sample temperature. The three separate linear trendlines were fitted to the curve. The activation barriers to chemisorption were found to be 13, 62, and 297 meV for low, mid, and high temperature ranges (100–175, 200–225, and 250–300 K), respectively.

$$S_0 = \alpha \frac{k_c}{k_c + k_d}, \tag{1}$$

$$k_i = \upsilon_i e^{(-E_1/k_h T_S)}, \tag{2}$$

thus,

$$\ln \frac{\alpha - S_0}{S_0} = \ln \frac{\upsilon_d}{\upsilon_c} - \frac{E_d - E_c}{k_b T_S}, \tag{3}$$

where S_0 is the probability a chemisorption event occurs, α is the probability NO physisorbs to the surface upon collision, k_c and k_d represent the chemisorption and desorption rate coefficients, respectively, ν_i is the preexponential term, and E_i is the activation energy. It is assumed that every molecule that impinges on the surface physisorbs, α=1. Although this may not be a realistic assumption, especially at high temperature, varying α only changes the barrier energies by 30% or less. By substituting and rearranging the equations, the barrier heights of the different pathways can be determined by plotting the initial sticking data as a function of inverse temperature.

Figure 8 is an Arrhenius plot of the initial sticking data for the 0.26 eV NO beam. The Arrhenius plot is nonlinear. By fitting the results to three separate linear trend lines, the barriers to chemisorption at low, mid, and high temperatures were determined. The data sets from the higher and lower incident beam energies gave similar results and are not shown. The barriers were found to be 15±2 meV at low temperatures (100–175 K), 61±10 meV at midtemperatures

(175–225 K), and 310±50 meV at high temperatures (250–300 K) for NO chemisorption, consistent with multiple distinct physisorption sites.

The ratio of the preexponential term, ν_d/ν_c, also varies for the three temperature ranges: 7–17 (100–175 K), $70-1\times10^3$ (175–225 K), and $1\times10^6-1\times10^9$ (250–300 K). Note that ν_d/ν_c represents the ratio of the preexponential kinetic parameters for conversion of physisorbates to desorbed molecules versus physisorbates to chemisorbed molecules assuming that the trapping probability is temperature independent. The low and the midrange temperature preexponential ratios are consistent with previous studies. Ferguson *et al.* found a ν_d/ν_c of 24 for the precursor-mediated sticking of O_2 on Si(100)-2×1.[17] Preexponential ratios greater than unity are physically reasonable due to higher entropy for desorption into the gas phase versus chemisorption on a surface. In Rettner and Mullins' study of O_2 on Pt(111), a ratio as great as 1000 was observed.[49] The low and the midrange temperature preexponential ratios are consistent with previous studies. However, for the high temperature ranges, ν_d/ν_c ranges from 1×10^6 to 1×10^9; this is greater than the ratio for different precursor-mediated chemisorption mechanisms of systems studied previously.[17,49,50] This suggests that the assumption of temperature independent trapping is not reasonable for NO/FePc above 250 K consistent with the shallow physisorption wells for NO/FePc.

The barriers to chemisorption are a function of temperature because there are many distinct physisorption sites with varying pathways to chemisorption. The distinct physisorption sites are the inner and outer ring nitrogen and peripheral carbons, a total of 7 different sites. Although simulations suggest that the physisorption sites have degenerate energies, the pathways between the physisorption sites to the metal center vary. Therefore, the barrier to chemisorption being a strong function of temperature is consistent with the barriers to diffusion being a strong function of the physisorption site.

IV. CONCLUSION

The surface reaction dynamics of NO onto a monolayer FePc thin film was explored. The initial sticking probability was found to be a function of incident molecular beam translational energy E_i and sample temperature T_s. NO adsorption onto FePc saturates at 3% of a monolayer at all incident beam energies (0.09–0.4 eV) and a large range of surface temperatures (100–200 K), consistent with the final chemisorption site being confined to the Fe metal centers. Control experiments performed on monolayer films of H_2Pc, which does not contain a metal center, showed zero chemisorption consistent with the necessity of the Fe metal centers to the chemisorption reaction mechanism. In contrast to NO/FePc saturation coverage, at low T_s and low E_i, the initial sticking probability for NO/FePc is as great as 40% and decreases linearly with increasing beam energy and surface temperature. These results are consistent with NO sticking onto the monolayer FePc via physisorption to the aromatic periphery followed by diffusion to the Fe metal center. A simple Arrhenius analysis is used to describe how the NO molecule adsorbs via a multiple pathway precursor-mediated chemisorption mechanism.

ACKNOWLEDGMENTS

The authors would like to thank the AFOSR-MURI (Grant No. F49620-02-1-0288) and the NSF (Grant No. CHE-0350571) for funding as well as the U.S. Department of Homeland Security Scholarship and Fellowship program for funding Ngoc L. Tran and the SRC AMD Graduate Fellowship for funding Sarah Bishop.

[1] G. Guillaud, J. Simon, and J. P. Germain, Coord. Chem. Rev. **180**, 1433 (1998).
[2] M. Bouvet, G. Guillaud, A. Leroy, A. Maillard, S. Spirkovitch, and F. Tournilhac, Sens. Actuators B **73**, 63 (2001).
[3] M. Bouvet, A. Leroy, J. Simon, F. Tournilhac, G. Guillaud, P. Lessnick, A. Maillard, S. Spirkovitch, M. Debliquy, A. de Haan, and A. Decroly, Sens. Actuators B **72**, 86 (2001).
[4] B. Bott and T. A. Jones, Sens. Actuators **5**, 43 (1984).
[5] R. Strohmaier, C. Ludwig, J. Petersen, B. Gompf, and W. Eisenmenger, J. Vac. Sci. Technol. B **14**, 1079 (1996).
[6] X. Lu and K. Hipps, J. Phys. Chem. B **101**, 5391 (1997).
[7] X. Lu, K. Hipps, X. Wang, and U. Mazur, J. Am. Chem. Soc. **118**, 7197 (1996).
[8] K. Hipps, X. Lu, X. Wang, and U. Mazur, J. Chem. Phys. **100**, 11207 (1996).
[9] D. E. Barlow and K. W. Hipps, J. Phys. Chem. B **104**, 5993 (2000).
[10] D. E. Barlow, L. Scudiero, and K. W. Hipps, Langmuir **20**, 4413 (2004).
[11] J. D. Wright, Prog. Surf. Sci. **31**, 1 (1989).
[12] Y. Sadaoka, Y. Sakai, N. Yamazoe, and T. Seiyama, Denki Kagaku oyobi Kogyo Butsuri Kagaku **50**, 457 (1982).
[13] C. R. Arumainayagam and R. J. Madix, Prog. Surf. Sci. **38**, 1 (1991).
[14] E. S. Hood, B. H. Toby, and W. H. Weinberg, Phys. Rev. Lett. **55**, 2437 (1985).
[15] M. Grunze, G. Strasser, and M. Golze, Appl. Phys. A: Solids Surf. **44**, 19 (1987).
[16] J. K. Brown and A. C. Luntz, Chem. Phys. Lett. **204**, 451 (1993).
[17] B. A. Ferguson, C. T. Reeves, and C. B. Mullins, J. Chem. Phys. **110**, 11574 (1999).
[18] M. P. Develyn, H. P. Steinruck, and R. J. Madix, Surf. Sci. **180**, 47 (1987).
[19] D. C. Seets, M. C. Wheeler, and C. B. Mullins, J. Vac. Sci. Technol. A **14**, 1566 (1996).
[20] J. E. Davis, S. G. Karseboom, P. D. Nolan, and C. B. Mullins, J. Chem. Phys. **105**, 8362 (1996).
[21] M. Hirsimaki and M. Valden, J. Chem. Phys. **114**, 2345 (2001).
[22] E. W. Kuipers, M. G. Tenner, A. W. Kleyn, and S. Stolte, Phys. Rev. Lett. **62**, 2152 (1989).
[23] A. J. Komrowski, K. Ternow, B. Razaznejad, B. Berenbak, J. Z. Sexton, I. Zoric, B. Kasemo, B. I. Lundqvist, S. Stolte, A. W. Kleyn, and A. C. Kummel, J. Chem. Phys. **117**, 8185 (2002).
[24] B. Berenbak, B. Riedmuller, D. A. Butler, C. T. Rettner, D. J. Auerbach, S. Stolte, and A. W. Kleyn, Phys. Chem. Chem. Phys. **2**, 919 (2000).
[25] J. Harris and A. C. Luntz, J. Chem. Phys. **91**, 6421 (1989).
[26] J. F. Zhu, M. Kinne, T. Fuhrmann, R. Denecke, and H. P. Steinruck, Surf. Sci. **529**, 384 (2003).
[27] D. A. King and M. G. Wells, Surf. Sci. **29**, 454 (1972).
[28] D. A. King and M. G. Wells, Proc. R. Soc. London, Ser. A **339**, 245 (1974).
[29] T. F. Hanisco, C. Yan, and A. C. Kummel, J. Chem. Phys. **97**, 1484 (1992).
[30] T. F. Hanisco, C. Yan, and A. C. Kummel, J. Phys. Chem. **96**, 2982 (1992).
[31] J. C. Buchholz and G. A. Somorjai, J. Chem. Phys. **66**, 573 (1977).
[32] I. Chizhov, G. Scoles, and A. Kahn, Langmuir **16**, 4358 (2000).
[33] T. Gopakumar, M. Lackinger, M. Hackert, F. Muller, and M. Hietschold, J. Phys. Chem. B **108**, 7839 (2004).
[34] H. Haberland, U. Buck, and M. Tolle, Rev. Sci. Instrum. **56**, 1712 (1985).
[35] M. Brandt, H. Muller, G. Zagatta, O. Wehmeyer, N. Bowering, and U.

Heinzmann, Surf. Sci. **333**, 30 (1995).
[36] T. F. Hanisco, C. Yan, and A. C. Kummel, J. Vac. Sci. Technol. A **11**, 2090 (1993).
[37] D. R. Miller, in *Atomic and Molecular Beam Methods*, edited by G. Scoles (Oxford University Press, New York, 1988), p. 14.
[38] B. Tsipinyuk, A. Budrevich, and E. Kolodney, J. Phys. Chem. **100**, 1475 (1996).
[39] B. Berenbak, D. A. Butler, B. Riedmuller, D. C. Papageorgopoulos, S. Stolte, and A. W. Kleyn, Surf. Sci. **414**, 271 (1998).
[40] A. M. Wodtke, H. Yuhui, and D. J. Auerbach, Chem. Phys. Lett. **413**, 326 (2005).
[41] N. L. Tran and A. C. Kummel, J. Chem. Phys. **127**, 214701 (2007).
[42] *CRC Handbook of Chemistry and Physics Internet Version 2007*, 87th ed., edited by D. R. Lide (Taylor & Francis, Boca Raton, FL, 2007).
[43] A. Hellman, B. Razaznejad, and B. I. Lundqvist, Phys. Rev. B **71**, 205424 (2005).
[44] C. Resch, V. Zhukov, A. Lugstein, H. F. Berger, A. Winkler, and K. D. Rendulic, Chem. Phys. **177**, 421 (1993).
[45] J. K. Brown, A. C. Luntz, and P. A. Schultz, J. Chem. Phys. **95**, 3767 (1991).
[46] B. Berenbak, B. Riedmuller, S. Stolte, and A. W. Kleyn, Chem. Phys. **301**, 309 (2001).
[47] M. Asscher, E. Pollak, and G. A. Somorjai, Surf. Sci. **149**, 146 (1985).
[48] P. D. Nolan, B. R. Lutz, P. L. Tanaka, J. E. Davis, and C. B. Mullins, J. Chem. Phys. **111**, 3696 (1999).
[49] C. T. Rettner and C. B. Mullins, J. Chem. Phys. **94**, 1626 (1991).
[50] D. C. Seets, M. C. Wheeler, and C. B. Mullins, Chem. Phys. Lett. **257**, 280 (1996).